Stability, Control, and Power Flow in Ad Hoc DC Microgrids

Wardah Inam, Julia A. Belk, Konstantin Turitsyn, David J. Perreault
Massachusetts Institute of Technology, Cambridge, MA, US
wardah@mit.edu, jabelk@mit.edu, turitsyn@mit.edu and djperrea@mit.edu

***Abstract*—Lack of access to electricity continues to plague more than one billion people. Microgrids which could be set up with limited planning would allow underserved communities to participate in energy markets without central oversight, but preexisting stability criteria and control techniques are ill-suited to this kind of network. We focus on the stability and control of networks formed by the ad hoc interconnection of modular power sources and loads. Equilibrium point feasibility—a minimum node voltage and minimum distribution efficiency—can be guaranteed by placing upper bounds on the droop and line resistances. Small-signal stability of the equilibrium point can be guaranteed by including a minimum capacitance (often already present) at the input of each load converter. We derive closed-form expressions for each of these bounds. Additionally, we present experimental validation of a new, multipurpose, secondary microgrid control scheme. The proposed method improves voltage regulation and power sharing—eliminating the steady-state power sharing error inherent to previous methods.**

I. Introduction

In regions with underfunded or nonexistent centralized power systems—like many developing countries—decentralized and scalable electrical networks would be very valuable. More than one billion people remain without any electricity access and many more have only unreliable service; this shortfall dramatically impedes human development [1]. Universal access has not been realized because underserved communities are often geographically remote and/or lack economic/political influence [2]. These barriers can be overcome by microgrids, which, compared to installing isolated generation at each home (e.g., solar home systems), can increase reliability and decrease costs by having multiple power sources connected to the same network. However, an ongoing impediment to the large-scale deployment of microgrids is the specialized planning required for each community. In this paper, we focus on a new type of microgrid which significantly reduces the amount of planning required: ad hoc dc microgrids.

Ad hoc microgrids are different from conventional microgrids because the network topology is not determined beforehand. They are formed by the ad hoc interconnection of modular sources and loads. Once connected, the sources communicate to autonomously perform the duties of the system operator in a traditional power system: forecasting, scheduling, and dispatching power. Accordingly, individuals can own a source and/or load module which, when connected in a network with other modules, automatically manages power usage and balances supply and demand in real time. Because the network is designed to be set up by non-expert community members, as opposed to a specialized team, the modules must be designed such that *any interconnection* will function appropriately.

978-1-5090-1815-4/16/$31.00

We focus on a dc microgrid presented previously [3]. DC microgrids are especially suited to off-grid electrification because of the widespread use of inherently-dc sources and loads (solar panels, batteries, phones) and the advent of low-cost, high-efficiency, dc-dc power converters [3]. In this paper, we use "source" to describe the combination of a power source, power converter to interface with the network, and communication/control unit. Likewise, "load" refers to a power load and an associated power converter/control unit. Since droop control is employed we model sources as Thevenin sources (a resistor and ideal voltage source in series). Due to the use of tightly-regulated power converters with each device, loads are modeled as ideal constant power sinks.

To evaluate the existence and feasibility of the network equilibrium point (Section III), we reduce "any arbitrary topology" to a "worst-case topology" and develop closed-form upper bounds on the droop and line resistances such that these constraints are met. For small-signal stability (Section IV), we linearize our models and use a state-space approach to find that stability can be guaranteed by ensuring a minimum capacitance at the input of each load, which is often already present in the input filter of the load converter. A previous attempt at state-space analysis of general networks used identical models and a similar technique, but is ultimately not reflective of practical networks because standalone sources or loads are not acceptable; they must come in pairs [4]. Other previous work on microgrid stability has been based on the Middlebrook Criterion (originally developed for input filter design) [5], [6]. Middlebrook-based techniques typically do not assume timescale separation between the converter and the network, which is necessary for filter design, but not always useful for the analysis of multi-converter networks. Accordingly, the analysis depends heavily on the specific converter implementation and equivalent network model, which is labor intensive and difficult to generalize. By contrast, we obtain a single closed-form expression for the load input capacitance which can be quickly and easily checked for any network. Hence, our conditions are more tractable, less complex, and more flexible than previous stability criteria.

In addition to guaranteeing network stability, it is also useful to control the power flows and voltage levels in the network. In theory, achieving accurate power dispatch and voltage regulation is not difficult, and several suitable methods have been proposed [7], [8], [9], [10], [11]. However, many of these methods have not been experimentally validated and do not account for critical nonidealities (e.g., communication delays) [7], [8], [9]. In practice, primary (droop) control remains the technique most commonly used for power sharing and secondary control is used to restore the network voltage [12]. Accurate power sharing is principally be achieved through the use of very large droop gains (r_d, see Fig. 1) relative to the line resistance, which, as discussed further in Section III, is often not acceptable. To achieve acceptable voltage regulation in the transient and precise power sharing in steady-state, in Sections V and VI we propose and experimentally validate a new, multipurpose, secondary controller. The key difference from conventional methods is that, in the proposed method, each open source reference voltage can vary independently (via δ_k—see Fig. 1c) . Multipurpose control can accurately realize any desired power dispatch—allowing, for example, a source to supply no power without disconnecting or a battery to either charge from or discharge to the network, which is not possible with conventional methods. This capability is a prerequisite for efficient and economically-optimal power dispatch.

In summary, the two main contributions of this paper are:

1) developing conditions on individual modules which can guarantee the existence, feasibility, and small-signal stability of an equilibrium point of any network, and
2) formulating and experimentally validating a new method of secondary microgrid control to physically realize accurate power dispatch—allowing each source to set and update the fraction of total power that it supplies.

II. Microgrid Architecture and Models

In this section we present the models chosen to represent the sources, loads, and lines. It is assumed that there is timescale separation between the internal converter dynamics and the network dynamics, which allows the use of analytically tractable and general models that can be adapted to describe many converters: droop-controlled voltage sources and constant power loads.

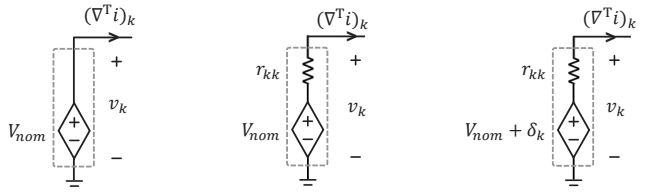

(a) Internal control only.

(b) Primary control added.

(c) Secondary control added.

Figure 1: Source model with successive levels of hierarchical control. v_k is the converter output voltage. The model with primary control is used for stability analysis (Sections III and IV); secondary control is discussed in Sections V and VI.

A. Hierarchically-Controlled Sources

The model used to represent the source depends on the control scheme used, as shown in Fig. 1. The function of each control mechanism is briefly summarized here and discussed further in Section V. Internal control refers to the standard voltage and/or current control loops inside each converter which do not require communication and—for voltage-source converters—realizes $v_k = V_{nom}$. Primary (droop) control varies the output voltage of each converter proportionally to the output current, mimicking a resistor r_d (shown as r_{kk} in Fig. 1b). Primary control causes v_k to deviate from the nominal voltage V_{nom}, but allows each converter to control its power output. To mitigate the network voltage deviation caused by primary control, secondary control is used to increment the reference voltage of each converter by δ_k. There are many methods of calculating δ_k, [11], [13]—in Section V we discuss two: the standard method [12] and our proposed multipurpose method.

Secondary control requires communication. In our system, communication occurs much more slowly than network dynamics (yielding two degrees of timescale separation, from slowest to fastest: secondary control, network dynamics, and converter dynamics), so in the following sections we will use a droop controlled source (Fig. 1b) to evaluate existence, feasibility, and stability of an equilibrium point. Stability of the secondary controller is an additional question, on top of the stability of the underlying network, which is outside the scope of this work.

B. Loads

The load is modeled as a constant power load (CPL) in parallel with a capacitor, shown in Fig. 2. Using a CPL is a conservative choice because it represents a perfectly regulated power converter with infinite control bandwidth [14]. The parallel capacitor represents the input capacitance of the load converter and, as shown in Section IV, can be used to ensure stability. Capacitors used for this purpose typically have non-zero parasitic resistance which tends to improve system stability margins, but we exclude that resistance here.

C. Interconnecting Lines

The sources and loads are connected by lines modeled by resistors and inductors as shown in Fig. 3.

D. Defining an Ad Hoc Microgrid

To guarantee appropriate operation, in Sections III and IV we will solve for bounds on each of three free parameters that certify a set of constraints will be met—independent of the configuration of the network. The parameters and constraints we have chosen are summarized here.

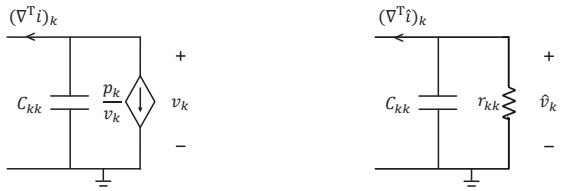

(a) Nonlinear. (b) Linearized.

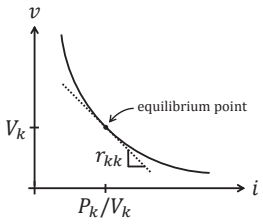

(c) CPL current-voltage characteristic.

Figure 2: Load model. Constant power load with input capacitance. Linearized model used for small signal analysis: $r_{kk} = -V_k^2/P_k$.

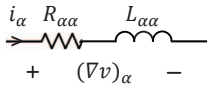

Figure 3: Line model.

1) Constraints:

- Minimum voltage V_{min}: all nodes in the network must be above this level.
- Minimum equilibrium distribution efficiency $\eta_{min} = P_{out}/P_{in}$ [1].
- Small-signal stability of the equilibrium point.

2) Given Parameters:

- s sources, l loads, and m lines
- Nominal network voltage V_{nom}
- Maximum aggregate load power $P_\Sigma = \max P_{out}$
- Line time constant $\tau = L_{\alpha\alpha}/R_{\alpha\alpha}$

3) Free Parameters:

- Load input capacitance C_{kk}
- Droop resistance: source r_{kk}
- Maximum resistance between a source and a load R_{max}

E. Mathematical Representation

Any network adhering to the constraints given above can be represented as a graph with $n = s + l$ nodes and m edges. We assume that the graph is strongly connected: that there is a path between every pair of nodes. We have used $x \approx X + \hat{x}$ to denote the small-signal variation $\hat{x}$ around the equilibrium point X.

We define matrices:

- $v \in \mathbb{R}^{n\times 1}$, a vector of node voltages.
- $i \in \mathbb{R}^{m\times 1}$, a vector of line currents.
- $R \in \mathbb{R}^{m\times m}$, a diagonal matrix with $R_{\alpha\alpha}$ equal to the resistance of line α.
- $L \in \mathbb{R}^{m\times m}$, a diagonal matrix with $L_{\alpha\alpha}$ equal to the inductance of line α.
- $r \in \mathbb{R}^{n\times n}$, a diagonal matrix with r_{kk} equal to the resistance from node k to ground. For source nodes, r_{kk} is the droop resistance, while for load nodes, $r_{kk} = -(V_k)^2/P_k$, the linearized constant power load resistance.
- $C \in \mathbb{R}^{n\times n}$, a diagonal matrix with C_{kk} equal to the capacitance from node k to ground. For source nodes, C_{kk} is a parasitic capacitance ($C_{kk} \to 0$), while for load nodes, C_{kk} is the converter input capacitance.
- $\nabla \in \mathbb{R}^{m\times n}$, an incidence matrix which defines the network topology. Row α has two nonzero elements: $\nabla_{\alpha s} = 1$ and $\nabla_{\alpha t} = -1$, with i_α defined as the current from source node s to target node t. Accordingly, $(\nabla v)_\alpha$ is equal to the voltage drop across line α, and $(\nabla^\top i)_k$ is equal to the total current flowing from ground out of node k.

Using these definitions, we can write the small-signal equations for any network configuration defined by ∇:

$$C\frac{d\hat{v}}{dt} + r^{-1}\hat{v} + \nabla^\top \hat{i} = 0\,, \tag{1}$$

$$L\frac{d\hat{i}}{dt} + R\hat{i} = \nabla\hat{v}\,. \tag{2}$$

For any pre-determined topology, these equations can be used to numerically check stability and equilibrium point feasibility. However, to design ad hoc systems, we want to pick the component values such that *any* ∇ will result in a system that has an appropriate equilibrium point. We explore that problem in the following sections.

III. Existence and Feasibility of Equilibrium

There are three components of network stability:

1) The existence of a feasible equilibrium point,
2) returning to the equilibrium point after small disturbances (small-signal stability), and
3) returning to the equilibrium point after large disturbances (large-signal stability).

In this section and the next we address 1) and 2) for ad hoc dc microgrids. Large-signal stability is outside the scope of this work.

A. "Worst-Case" Network Configuration

Existence of an equilibrium corresponds to the sources' ability to supply the demanded power. In addition, there are typically also tighter bounds specifying a minimum node voltage (V_{min}) and a minimum distribution efficiency (η_{min}).

[1] P_{out} is the total power drawn from the network (sum over nodes where $v_k(\nabla^\top i)_k$ is negative) and P_{in} is the total power put into the network (sum over nodes where $v_k(\nabla^\top i)_k$ is positive).

Although the configuration of an ad hoc network can be arbitrary, existence and feasibility of an equilibrium point can be certified by considering a "worst-case" configuration for a set of sources, lines, and loads, assuming the total load power is P_Σ and the maximum resistance between a source and a load is R_{max}. The highest distribution losses and maximum voltage deviation both occur when the loads and sources are maximally separated, as shown in Fig. 4. If restrictions are placed on the network topology, the worst-case may be further constrained, and the conditions may be relaxed. In this section we proceed with the most general "worst-case," and in Section VI-A we provide an example of relaxing the conditions for the "distributed star" topology.

B. Existence of Equilibrium

The network shown in Fig. 4 will have an equilibrium point (i.e. a real solution) if and only if:

$$R_{max} + r_{d,max} \leq \frac{V_{nom}^2}{4P_\Sigma}\,. \tag{3}$$

When (3) is binding, $V_2 = V_{nom}/2$ and the total power dissipated at the load is equal to the total power "dissipated" in the lines and droop resistance. In typical electrical networks, $V_{min} \gg V_{nom}/2$ and $\eta \gg 0.50$, so additional analysis is needed to ensure the feasibility of the equilibrium.

C. Feasibility of Equilibrium

There are two constraints—$\eta \geq \eta_{min}$ (η defined in II-D) and $V_i \geq V_{min} \quad \forall i$—which together determine the two free parameters in the system—R_{max} and $r_{d,max}$. First, we can use the minimum voltage level to bound the sum of the resistances. From Fig. 4, the voltage deviation constraint will be satisfied when:

$$R_{max} + r_{d,max} \leq \frac{V_{min}(V_{nom} - V_{min})}{P_\Sigma}\,. \tag{4}$$

Next, we can write down the distribution efficiency constraint:

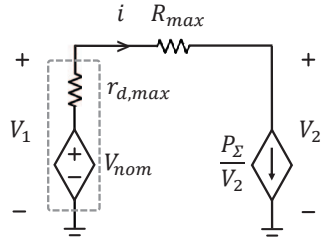

Figure 4: Configuration with highest distribution losses and voltage deviation shown in equilibrium. In terms of the existence and feasibility of an equilibrium point, the "worst-case" configuration that can be formed from a set of sources, lines, and loads defined as in Section II-D.

$$\eta_{min} \leq \frac{iV_2}{iV_1} = \frac{P_\Sigma}{\left(V_{nom} - \frac{P_\Sigma}{V_2} r_{d,max}\right)\frac{P_\Sigma}{V_2}}\,. \tag{5}$$

These constraints—(4) and (5)—can be reduced to explicit expressions for R_{max} and $r_{d,max}$ by noticing that both constraints will bind simultaneously and substituting $V_2 = V_{min}$ into (5). In this way, (4) can be used to find the maximum total resistance, and then (5) can be used to split the total allowable resistance into the line resistance and the droop resistance:

$$R_{max} \leq \frac{V_{min}^2(1 - \eta_{min})}{P_\Sigma \eta_{min}}\,, \tag{6}$$

$$r_{d,max} \leq \frac{V_{min}(\eta_{min} V_{nom} - V_{min})}{P_\Sigma \eta_{min}}\,. \tag{7}$$

Note that, because $r_{d,max}$ is an internal control parameter, it does not dissipate power. Accordingly, the efficiency will always be higher than the per unit voltage deviation: $\eta > V_2/V_{nom}$.

To summarize: given an ad hoc microgrid defined by a nominal voltage V_{nom}, a maximum total load P_Σ, and some constraints—V_{min} and η_{min}—as long as $V_{min} \geq V_{nom}/2$ an equilibrium point will exist for any network configuration and Eqs. (6) and (7) can be used to solve for the allowable line and droop resistances. If the network is overloaded and these constraints are not satisfied, load shedding can be used to ensure appropriate operation.

IV. Small-Signal Stability

In addition to feasibility, we also need to guarantee the stability of the equilibrium point. This is especially difficult for ad hoc networks for two reasons:

1) All loads are interfaced to the network via tightly-regulated power electronic converters and hence have a negative incremental impedance.
2) The network configuration is not predetermined, so we are seeking conditions on the individual units (sources/loads) such that the microgrid formed by *any interconnection* will be stable.

In this section we present a state-space approach that we have used to develop suitable conditions. We rely on both linearized models and the assumption that all lines in the network have the same time constant.

A. Simple Network

To demonstrate the approach, first consider the simple network shown in Fig. 5. A single source, load, and line are connected, with the load linearized around V_1 and drawing power P_1: $r_{cpl} = -V_1^2/P_1$. Applying the Routh-Hurwitz stability criterion to the network (equivalently, checking that the real part of each eigenvalue is negative), we obtain two necessary and sufficient conditions for small-signal stability:

$$C_i > \frac{L_l}{R_l + r_d}\frac{P_1}{V_1^2}\,, \tag{8}$$

$$\frac{V_1^2}{P_1} > R_l \,. \tag{9}$$

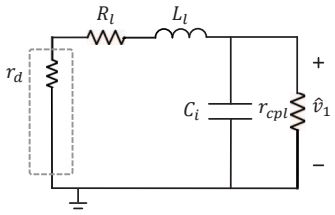

Figure 5: Simple system for demonstrating small-signal stability analysis.

B. General Formulation

The same approach can be used on an arbitrary network defined by the node and line state equations (1) and (2). Assuming that all lines have the same time constant $\tau = L_{\alpha\alpha}/R_{\alpha\alpha}$, (1) and (2) can be combined into one second order equation:

$$\tau C\ddot{\hat{v}} + (C + \tau r^{-1})\dot{\hat{v}} + (\nabla^\top R^{-1}\nabla + r^{-1})\hat{v} = 0\,. \tag{10}$$

Multiplying by $\dot{\hat{v}}^\top$ and rearranging:

$$\frac{d}{dt}\frac{1}{2}\left[\dot{\hat{v}}^\top \tau C\dot{\hat{v}} + \hat{v}^\top(\nabla^\top R^{-1}\nabla + r^{-1})\hat{v}\right] = \dot{\hat{v}}^\top\left[C + \tau r^{-1}\right]\dot{\hat{v}} \tag{11}$$

The stability of the network is guaranteed if the following necessary and sufficient conditions are satisfied:

1) The left side of (11) defines a convex Lyapunov function:

$$\tau C \succ 0\,, \tag{12}$$

which is trivially satisfied in realistic networks, and

$$\nabla^\top R^{-1}\nabla + r^{-1} \succ 0\,. \tag{13}$$

2) The right side of (11) is always negative:

$$C + \tau r^{-1} \prec 0\,. \tag{14}$$

If the network is completely pre-determined (i.e., the component values and topology are known beforehand), these matrix inequalities can be checked numerically. However, to design ad hoc systems, we need to reduce (13) and (14) to conditions on individual sources and loads.

C. Small Signal Stability: Condition 1 of 2

Equation (13) can be interpreted physically by noticing that, when multiplied by $\hat{v}^\top$ and $\hat{v}$, the first term corresponds to the power dissipated in the lines and the second term corresponds to the power dissipated in the loads. Informally, to be stable, the small signal model of the network must always dissipate positive power. This is trivial in systems with positive resistors, but is not necessarily satisfied in networks with constant power loads. Using a path decomposition argument, (13) can be reduced to (see [15] for the proof):

$$R_\Sigma + r_{d,max} \le \frac{V_{min}^2}{P_\Sigma}\,. \tag{15}$$

Note that this equation is always less restrictive than the minimum voltage constraint (Equation 4) when an equilibrium point exists (Equation 3 or equivalently $V_{min} > V_{nom}/2$).

D. Small Signal Stability: Condition 2 of 2

Equation (14) can be reduced by noting that, for a diagonal matrix D, $D \succ 0$ if and only if $D_{ii} > 0$ for all i. Accordingly, $\tau^{-1} + 1/(r_{kk}C_{kk}) > 0$ for all k.

For generator nodes this can be rewritten:

$$r_d C_{kk} > -\tau\,. \tag{16}$$

For positive droop resistances, this is trivially satisfied in the limit $C_{kk} \to 0$.

For load nodes, however, the condition is not always satisfied:

$$C_{kk} > \frac{\tau P_k}{(V_k)^2}\,. \tag{17}$$

This condition depends on the equilibrium node voltage V_k and equilibrium output power P_k, but can be further simplified by assuming $V_k \ge V_{min}$ and $P_k \le P_{k,max}$. Hence, each load capacitance must satisfy:

$$C_{kk} > \frac{\tau P_{k,max}}{V_{min}^2}\,. \tag{18}$$

V. Microgrid Control

In the previous sections, we have found conditions under which the microgrid, in the presence of internal and primary control, will have a stable equilibrium point. In addition, secondary control is often used to improve the performance of the network. For this discussion, we use the conventional definitions of the control levels: primary control consisting of a "virtual" (droop) resistor and secondary control consisting of an offset voltage δ_k, as shown in Fig. 1 [12]. Together, primary and secondary control are used to ensure three objectives:

1) **Limiting circulating currents:** when ideal voltage sources are connected in parallel through lines with small resistances, small mismatches in the source voltages V_{nom} can cause large circulating currents (e.g., an undesirably large current out of some source(s) and small or negative currents into others). Nonidealities make these mismatches inevitable, but these currents can be reduced by including additional resistance.
2) **Regulating the network voltage:** the devices connected to the network are designed to operate in a specified voltage range. Accordingly, all node voltages should remain near the nominal voltage V_{nom}. The desired voltage level does not change and should be maintained with or without communication.
3) **Dispatching power:** we would like each source to be able to set (and update) its fraction of total supplied

power. Each power source has a cost function that describes how "expensive" it is for that source to supply power (based on factors like the state-of-charge of the battery). To ensure that power is supplied at minimal cost, each time the optimal dispatch is computed, we need to physically realize the dispatch by coordinating the sources.

Typically, primary control is used to set the fraction of power each source supplies and secondary control is used to correct for the voltage deviation caused by primary control [12]. However, to accomplish power dispatch using only primary (proportional) control, very large droop resistances (relative to the line resistances) must typically be used. These large values of r_d cause large transient voltage deviations, meaning that, using the conventional method, there is an unavoidable trade off between power-sharing accuracy and transient voltage regulation. Further, maintaining appropriate node voltages is critical for converter operation, while accurate power dispatch is a nice—but not critical—feature.

To ensure all control objectives are met *even with* small r_d values, here we propose a new formulation of primary and secondary control. In our method, the network will function properly (maintaining all node voltages $\geq V_{min}$) in the absence of secondary control by designing r_d in accordance with the V_{min} constraint (Equation (7)). We use droop control only to limit circulating currents, so we set all r_d values equal to $r_{d,max}$ as defined by Equation (7). By contrast, in the conventional method, r_d must be updated to change power sharing proportions, which requires communication *anyway*. Our r_d values do not change, so our primary control is truly local, and power sharing proportions are determined by a new parameter, λ. Using λ we incorporate the power sharing objective into our secondary controller in addition to the voltage regulation objective.

First we define a voltage error:

$$e_v = V_{nom} - \bar{v} \tag{19}$$

which is the same for each source. $\bar{v}$ is the average node voltage of all sources—it could also be defined as the average node voltage (including loads), but here we assume that only sources have communication capabilities.

Next, we use λ to specify a desired fraction of total power that each source supplies. We define a power error:

$$e_{p,k} = \lambda_k \bar{p} - \bar{\lambda} p_k \tag{20}$$

which is *not* the same for each source. $\bar{p}$ and $\bar{\lambda}$ are p and λ averaged over the sources.

Together, these can be combined into an integral controller:

$$\frac{d}{dt}\delta_k = k_{i,v} e_v + k_{i,p} e_{p,k}\,. \tag{21}$$

Unlike the standard method of control, in our method, the δ_k's are not the same for all sources. The proposed strategy can realize arbitrary power sharing ratios—allowing, for example, one source to produce zero power without disconnecting, or batteries to charge from the network (setting $\lambda_{\text{battery}} < 0$ to charge, and > 0 to discharge. Our inclusion of primary control limits transient circulating currents while still maintaining adequate voltage regulation.

The controller can be discretized based on the messaging delay T_m:

$$\delta_k[t] = \delta_k[t - T_m] + T_m k_{i,v} e_v[t] + T_m k_{i,p} e_{p,k}[t]\,. \tag{22}$$

The implementation can be done in a centralized or distributed manner, depending on the communication configuration of the network. Either a central "master" node can receive the necessary information (voltage and current from each source), compute the δ_k's, and relay them back to the other sources, or source nodes can locally store the state of all other sources and perform the computations themselves.

In essence, for sources modeled as shown in Fig. 1, there are two control parameters: r_{kk} and δ_k. The traditional method updates r_{kk} to vary the power sharing proportions and updates δ_k to regulate the network voltage—both of which require communication. Our method fixes all r_{kk}'s to limit circulating currents and updates δ_k to achieve both power sharing and voltage regulation.

VI. Experimental Validation

Here we present validation of a microgrid that adheres to the constraints developed in previous sections, demonstrating power sharing accuracy in response to a load step. The test setup is a microgrid consisting of two source (boost) converters and seven load (flyback) converters connected as shown in Fig. 6 with parameters given in Table I. The converter systems are described in detail in [16]. First, we analyze the network in the context of the previously-determined constraints.

Table I: Network Specifications

Parameter	Value
Predetermined Parameters	
Network Configuration	Distributed Star
Number of Sources	2
Number of Loads	7
Nominal Voltage (V_{nom})	24 V
Total Load Power (P_Σ)	140 W
Max Line Time Constant (τ_{max})	0.27 ms
Constraints	
Min Node Voltage (V_{min})	18 V
Min Distribution Efficiency (η_{min})	90%
Free Parameters	
R Between Source and P_Σ (R_{max})	0.22 Ω($\leq$ 0.26Ω)
Droop Resistance (r_d)	0.50 Ω($\leq$ 0.51Ω)
Load Input Capacitance (C)	80 µF ($\geq$ 16.7 µF)
Control Parameters	
Time between messages (T_m)	1.5 s
Voltage gain ($k_{i,v}$)	0.30 $\text{V}^{-1}\,\text{s}^{-1}$
Power gain ($k_{i,p}$)	0.017 $\text{W}^{-1}\,\text{s}^{-1}$
Experiment: Line Impedances	
$Z_1 = R_1 + j\omega L_1$	0.83 Ω+ $j\omega$(18 µH)
$Z_2 = R_2 + j\omega L_2$	0.10 Ω+ $j\omega$(27 µH)

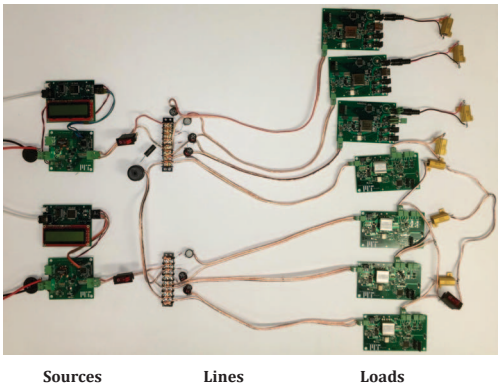

(a) Picture.

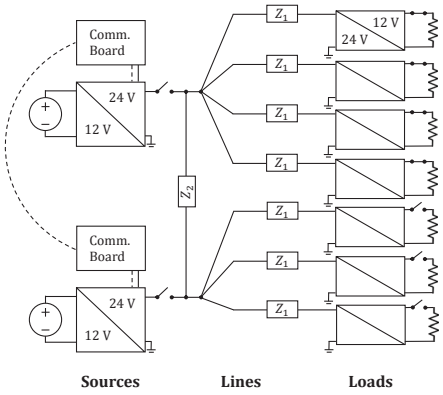

(b) Schematic.

Figure 6: Our experimental setup.

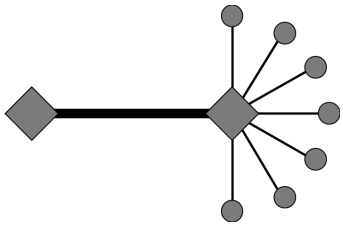

Figure 7: Two sources and seven loads connected in the worst case distributed star topology.

A. Designing a Sample Network

We begin by demonstrating how the conditions in the equilibrium point section can be relaxed by imposing some restrictions on the network topology. Here, we restrict ourselves to a "distributed star" network, where all sources are connected with lines of impedance $Z_2 = R_2 + j\omega L_2$ and all loads are connected to the nearest source with a line of impedance $Z_1 = R_1 + j\omega L_1$, as shown in Fig. 6. There are two sources and seven loads on the network, and each load is either off or on: $p_k \in \{0, 20\}\text{W}$. The "worst case" under these restrictions is shown in Fig. 7. Without any restriction on the configuration, $R_{max} = R_1 + R_2$ and $P_\Sigma = 140\,\text{W}$. However, in the configuration shown in Fig. 7, the 7 identical loads can reduced to a single equivalent load, reducing R_{max} to $R_1/7 + R_2$. Now, using the constraints derived in Section III, we can calculate allowable r_d, R_1, and R_2 values. The constraints and results are summarized in Table I.

B. Experimental Results

Our experimental results are shown in Fig. 8 and Fig. 9. In Fig. 8, $\lambda_1 = \lambda_2 = 1$, and the sources shared equally. In Fig. 8, $\lambda_1 = 1.2$, $\lambda_2 = 0.8$, and the sources realized the specified ratio. In both cases a small steady-state error is observed, which is smaller than the tolerance of our measurement equipment. The two largest sources of error are:

- Current sensor in each source converter (ACS711): $\pm 5\%$ accuracy.
- Oscilloscope current probe (TCP0030 and TCP202): $\pm 1\%$ accuracy.

In addition, small variations can be observed (especially in Fig. 8a—less than 5% deviation from the desired value) after the controller has largely settled—after approximately $8\,\text{s}$. These are caused by measurement noise, and could be eliminated by turning the controller off once the error is smaller than some threshold.

VII. Conclusion

Ad hoc dc microgrids have significant potential to address the ongoing and widespread lack of electricity in many regions. Because they are formed by the ad hoc interconnection of modular sources and loads, each module must be designed so that any interconnection will meet predetermined constraints. The network topology of conventional power systems is known beforehand, so conventional techniques are poorly-suited to the analysis of ad hoc networks. In this paper we have demonstrated how individual source and load modules can be designed to meet a particularly relevant set of constraints: existence, feasibility, and small-signal stability of the network equilibrium point. Our results are summarized by Equations (6), (7), and (18). In addition, we have proposed and validated a new, multipurpose, secondary control scheme which can achieve precise steady-state power sharing and is capable of realizing arbitrary power sharing proportions. Broadly, we have demonstrated the ability of a modular and reconfigurable microgrid to maintain stable operation, achieve dynamic power sharing, regulate the network voltage, and adhere to efficiency constraints without the need for central pre-planning or oversight.

References

[1] IEA, *World Energy Outlook 2013*. International Energy Agency, 2013.

[2] P. Alstone, D. Gershenson, and D. M. Kammen, "Decentralized energy systems for clean electricity access," *Nature Clim. Change*, vol. 5, pp. 305–314, Apr 2015. Perspective.

[3] W. Inam, D. Strawser, K. Afridi, R. Ram, and D. Perreault, "Architecture and system analysis of microgrids with peer-to-peer electricity sharing to create a marketplace which enables energy access," in *Power Electronics and ECCE Asia (ICPE-ECCE Asia), 2015 9th International Conference on*, pp. 464–469, June 2015.

[4] S. Anand and B. G. Fernandes, "Reduced-order model and stability analysis of low-voltage dc microgrid," *Industrial Electronics, IEEE Transactions on*, vol. 60, pp. 5040 – 5049, November 2013.

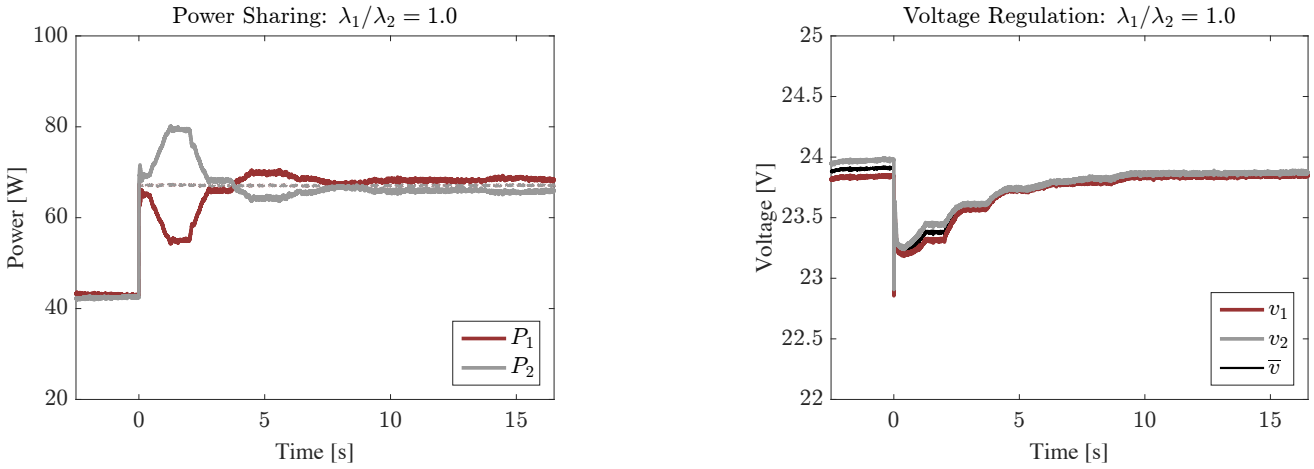

(a) (b)

Figure 8: Experimental demonstration of equal power sharing accurate to within the precision of our equipment.

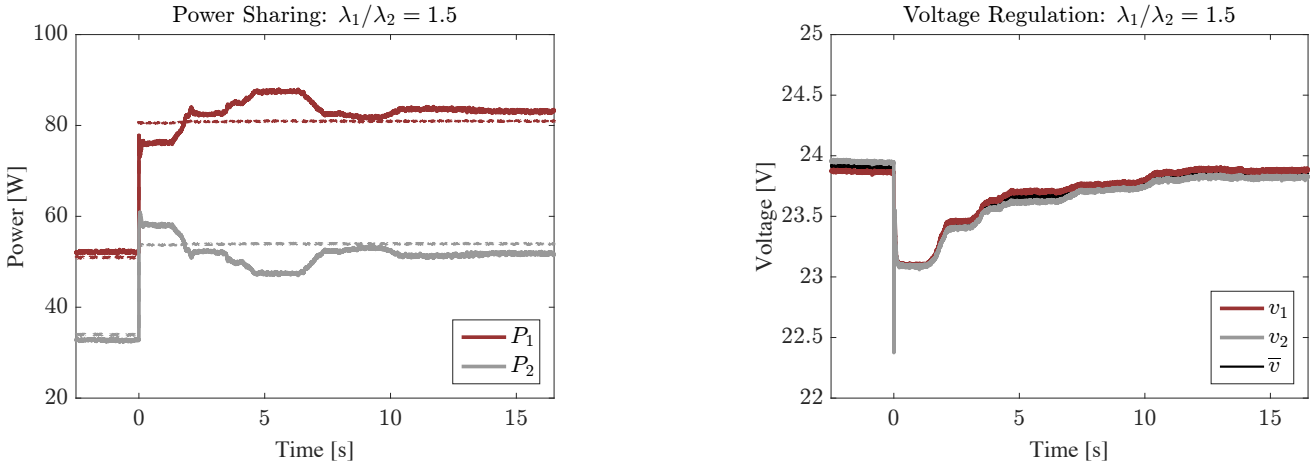

(a) (b)

Figure 9: Experimental demonstration of realizing a specified, unequal, power sharing ratio accurate to within the precision of our equipment.

[5] T. Dragievi, X. Lu, J. C. Vasquez, and J. M. Guerrero, "Dc microgrids part i: A review of control strategies and stabilization techniques," *IEEE Transactions on Power Electronics*, vol. 31, pp. 4876–4891, July 2016.

[6] A. Riccobono and E. Santi, "Comprehensive review of stability criteria for dc power distribution systems," *Industry Applications, IEEE Transactions on*, vol. 50, pp. 3525–3535, March 2014.

[7] J. Zhao and F. Dörfler, "Distributed control and optimization in dc microgrids," *Automatica*, vol. 61, pp. 18–26, 2015.

[8] C. Li, T. Dragicevic, N. L. Diaz, J. C. Vasquez, and J. M. Guerrero, "Voltage scheduling droop control for state-of-charge balance of distributed energy storage in dc microgrids," in *Energy Conference (ENERGYCON), 2014 IEEE International*, pp. 1310–1314, May 2014.

[9] T. Morstyn, B. Hredzak, V. G. Agelidis, and G. Demetriades, "Cooperative control of dc microgrid storage for energy balancing and equal power sharing," in *Power Engineering Conference (AUPEC), 2014 Australasian Universities*, pp. 1–6, Sept 2014.

[10] S. Anand, B. Fernandes, and M. Guerrero, "Distributed control to ensure proportional load sharing and improve voltage regulation in low-voltage dc microgrids," *Power Electronics, IEEE Transactions on*, vol. 28, pp. 1900–1913, April 2013.

[11] X. Lu, J. Guerrero, K. Sun, and J. Vasquez, "An improved droop control method for dc microgrids based on low bandwidth communication with dc bus voltage restoration and enhanced current sharing accuracy," *Power Electronics, IEEE Transactions on*, vol. 29, pp. 1800–1812, April 2014.

[12] J. Guerrero, J. Vasquez, J. Matas, L. de Vicua, and M. Castilla, "Hierarchical control of droop-controlled ac and dc microgridsa general approach toward standardization," *Industrial Electronics, IEEE Transactions on*, vol. 58, pp. 158–172, January 2011.

[13] P. H. Huang, P. C. Liu, W. Xiao, and M. S. E. Moursi, "A novel droop-based average voltage sharing control strategy for dc microgrids," *IEEE Transactions on Smart Grid*, vol. 6, pp. 1096–1106, May 2015.

[14] A. Emadi, A. Khaligh, C. H. Rivetta, and G. A. Williamson, "Constant power loads and negative impedance instability in automotive systems: definition, modeling, stability, and control of power electronic converters and motor drives," *Vehicular Technology, IEEE Transactions on*, vol. 55, pp. 1112–1125, July 2006.

[15] J. A. Belk, W. Inam, D. J. Perreault, and K. Turitsyn, "Stability and Control of Ad Hoc DC Microgrids," *arXiv.org*, Mar. 2016.

[16] W. Inam, *Adaptable Power Conversion for Grid and Microgrid Applications*. PhD thesis, Massachusetts Institute of Technology, 2016.